N. Goldstein; B. St. Peter; J. Grot; M. Kogan; M. Fox; P. Vujkovic-Cvijin; R. Penny; J. Cline, Portable, stand-off spectral imaging camera for detection of effluents and residues, SPIE 9482, Next-Generation Spectroscopic Technologies VIII, 94820X (3 June 2015).

doi: 10.1117/12.2179045

See next page.

Portable, stand-off spectral imaging camera for detection of effluents and residues

Neil Goldstein*, Benjamin St Peter, Jonathan Grot, Michael Kogan, Marsha Fox,
Pajo Vujkovic-Cvijin, Ryan Penny, and Jason Cline
Spectral Sciences Inc., 4 Fourth Ave, Burlington, MA 01803

ABSTRACT

A new, compact and portable spectral imaging camera, employing a MEMs-based encoded imaging approach, has been built and demonstrated for detection of hazardous contaminants including gaseous effluents and solid-liquid residues on surfaces. The camera is called the Thermal infrared Reconfigurable Analysis Camera for Effluents and Residues (TRACER). TRACER operates in the long wave infrared and has the potential to detect a wide variety of materials with characteristic spectral signatures in that region. The 30 lb. camera is tripod mounted and battery powered. A touch screen control panel provides a simple user interface for most operations. The MEMS spatial light modulator is a Texas Instruments Digital Microarray Array with custom electronics and firmware control. Simultaneous 1D-spatial and 1D-spectral dimensions are collected, with the second spatial dimension obtained by scanning the internal spectrometer slit. The sensor can be configured to collect data in several modes including full hyperspectral imagery using Hadamard multiplexing, panchromatic thermal imagery, and chemical-specific contrast imagery, switched with simple user commands. Matched filters and other analog filters can be generated internally on-the-fly and applied in hardware, substantially reducing detection time and improving SNR over HSI software processing, while reducing storage requirements. Results of preliminary instrument evaluation and measurements of flame exhaust are presented.

Keywords: Thermal infrared chemical contrast imaging spectral hyperspectral DMA

1. INTRODUCTION

Spectrally-resolved thermal contrast imagery can be used for visualization, detection, and quantification of chemical species through their characteristic long-wave infrared (LWIR) spectral signatures. Unfortunately, the high cost of two-dimensional array detectors has hampered the routine application of LWIR Hyperspectral Imaging (HSI) technology. We report here the practical implementation of a portable, and relatively low-cost thermal contrast imager using a single-element detector and a Digital-Micromirror Array (DMA) to perform both hyperspectral and chemical imaging, the latter based on creation of chemical-specific contrast images. A prototype sensor called TRACER (Thermal infrared, Reconfigurable, Analysis Camera for Effluents and Residues) was built specifically for application to explosive residue detection.[1,2] In this work we demonstrate its operation for other applications, including monitoring of the gaseous effluent from a flame.

Pictures of TRACER are shown in Figure 1. The optical system is based on an earlier laboratory breadboard sensor,[3,4,5] which uses a set of two concave gratings, a DMA, and Hadamard multiplexing to encode spectral and spatial data onto a single element detector. The detector waveform is then decoded to produce spectral imagery. The sensor may operate in hyperspectral imaging mode; however its strength lies in producing chemical-specific contrast images by implementing spectral transmission filter functions in hardware using grey scales on the DMA. Any linear spectral detection algorithm can be implemented using a small number of spectral filter masks. In this work we demonstrate the application of matched filters, but other linear detection algorithms such as orthogonal subspace projection, and principal component analysis could also be implemented using the on-board data system. The TRACER instrument contains an internal computer and storage system that allows it to collect and store spectra, maintain spectral libraries, and implement specialized analog spectral filters. Filters can be adapted to the application by including location and application specific background spectra in the filter generation process.

* neil@spectral.com; phone 1 781 273-4770; fax 1 781 270-1161; spectral.com

Figure 1. TRACER Contrast Imager Front (left) and Rear (right) Showing Touch-Screen Interface.

2. SYSTEM DESCRIPTION

TRACER is a self-contained imaging system comprising an optical bench, electronics, firmware, and software for creating contrast images based on spectral encoding. The method of operation is shown in Figure 2, which schematically represents the optical system, firmware for controlling the optics, and the software-based system control.

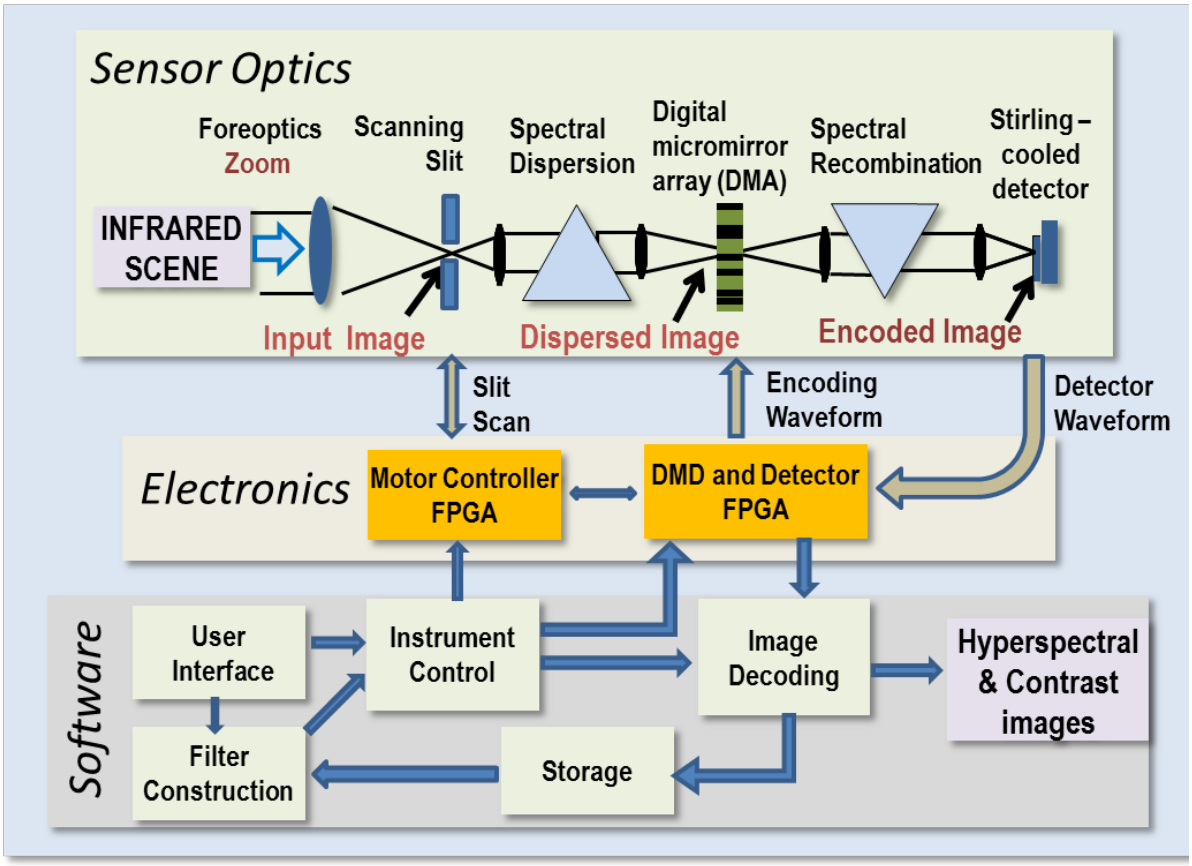

Figure 2. Schematic representation of the TRACER imaging system.

The optical system begins with an infrared, imaging-forming lens and ends with a closed-cycle, Stirling-cooled detector. Between the input image and the detector is an encoding system that disperses the light onto a DMA, encodes specific spectral and spatial aspects of the image, and then recombines the light into an encoded polychromatic image on the detector. The encoding system consists of two concave grating spectrographs with a DMA at their common focus. The first spectrograph is equipped with a vertically oriented scanning slit at the input image plane. For any given slit position, the spectrograph produces a dispersed image on the DMA, with one spatial axis along the slit dimension, and the spectral axis perpendicular to the slit. The DMA is programmed with a series of encoding masks that reflect specific spectral and spatial image regions through the second spectrograph for subsequent reimaging on the detector. The DMA cycles through the masks at a rate of 20 kHz producing an encoded waveform at the detector which contains information about the spatial and spectral distribution of the input image. This waveform is decoded in processing to reconstruct the dispersed spatial/spectral image on the DMA. The second spatial dimension is produced by scanning the input slit.

A custom electronics board with FPGA-based controller is used to synchronize the DMA and detector operation. The DMA control firmware generates masks that instruct individual DMA mirrors to turn on or off, loads them onto the DMA, and samples the detector output in a synchronous fashion at 20 kHz. A separate motor controller positions the slit. The two controllers use hardware handshaking to synchronize their activities. The TRACER enclosure also includes power conditioners, ancillary support electronics and two externally-mounted battery packs. It draws approximately 65 watts and can operate on battery power for more than two hours.

The software system, which resides on the embedded computer, handles the user interface, data storage, preparation of appropriate DMA masks and decoding of the detector waveforms to reconstruct hyperspectral and contrast imagery. Typically, Hadamard transform encoding is used for the spatial dimension and spectral matched filters are used for the spectral dimension. Alternatively, hyperspectral imagery is collected using Hadamard transform encoding for both the spatial and spectral dimensions. These methods are described in detail below. Spatial and spectral resolution and chemicals of interest can be selected by the user from the touch-screen display interface. Spectral and image data can be stored on board, and new spectral contrast filters can be created based on chemicals of interest, and location-specific spectral backgrounds.

3. OPTICAL BENCH

The optical bench is built on a space frame structure which integrates the scanning slit structure, DMA, concave gratings, and detector, and locates them precisely in space, based on machine tolerances. Figure 3 shows a side view of the optical structure (right) side by side with a ZEMAX optical design program schematic of the optics (left). The two spectrograph gratings are mounted on the floor plate. All other optics are mounted to the top plate. Note in the photo that a protective cover is placed over the gratings to protect them during the assembly process. The schematic includes a ray trace of the principal ray through the system for three wavelengths (7.1, 9.5, and 12.3 μm). Both side and bottom views are shown. The 3-dimensional light path through the optics is as follows: light enters from the left hand side, where the IR zoom lens (not shown) produces an image of the scene at the input slit. The light passes through the slit and is reflected by a turning mirror onto grating 1, which disperses the light to form a dispersed image on the DMA. The DMA deflects the selected spatial and spectral elements of the image onto grating 2, which reverses the dispersion of grating 1 and forms a recombined panchromatic image. A set of two lenses and two turning mirrors are used to reimage the light onto a cooled detector. The reimaging lenses produce a de-magnified image of the 4x4 mm field of view onto the 2x2 mm detector. The magnification factor is 1:2.2. A cold stop within the detector housing is placed at the image of the camera aperture stop. The resulting detector angular acceptance is 1.3 steradians. Because of the 2.2x image magnification the overall system F number is F/1.8.

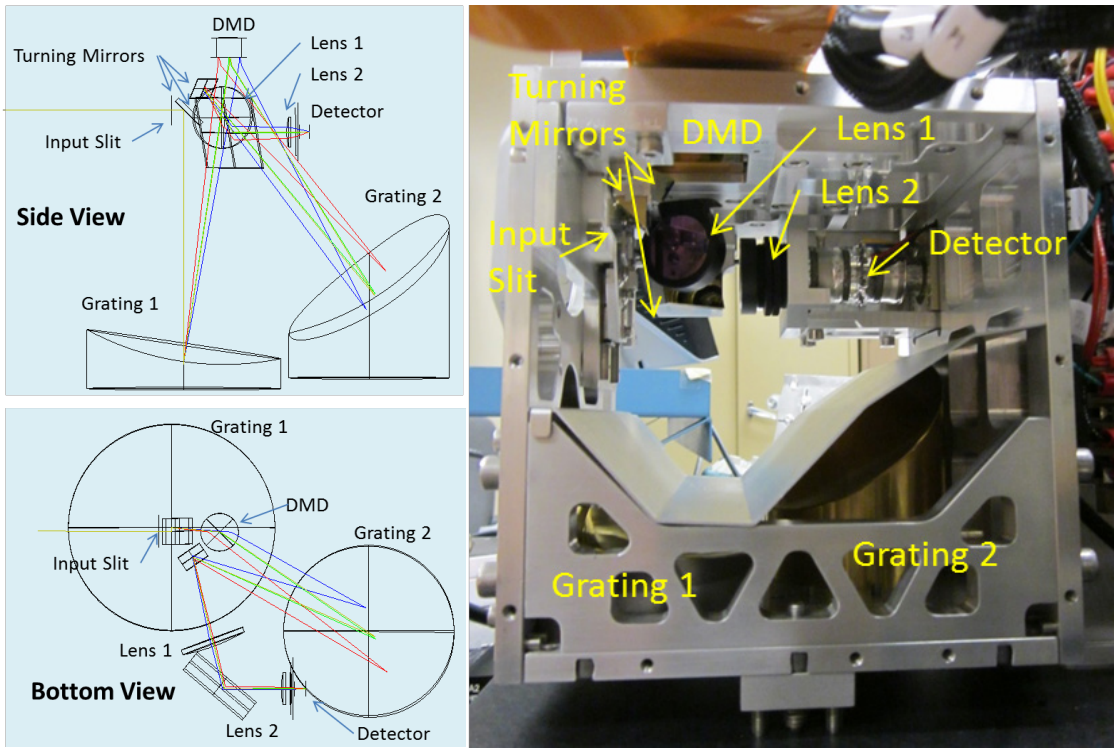

Figure 3. Elements of the optical system. Left – ZEMAX schematic. Right – photo of optics as built.

Figure 4 and shows spot diagrams for the image fields at the DMA (a) and on the detector (b) as computed in ZEMAX. Spots are shown for the center and the corners of the 4x4 mm field of view optical system and for three LWIR wavelengths in the absence of the slit. Figure 4a shows the dispersed image extended across the DMA. Each 2-dimensional monochromatic image would be 4x4 mm in size on the DMA. Light from each point in the image is dispersed across 9 mm of the14 mm long DMA. The input image spots are well resolved with rms spot radii of order 50 µm throughout the field of view. This blur spot, along with the slit width of 300 microns establishes the spatial resolution of the imaging system. Figure 4b shows the recombined image spots on the 2x2 mm detector after passing through the second grating and reimaging optics. The second grating recombines all wavelengths onto the 2x2 mm detector. There is some fall off at the corners as demonstrated in Figure 5, which shows the observed intensity distribution in the 9µm band as a function of field of view.

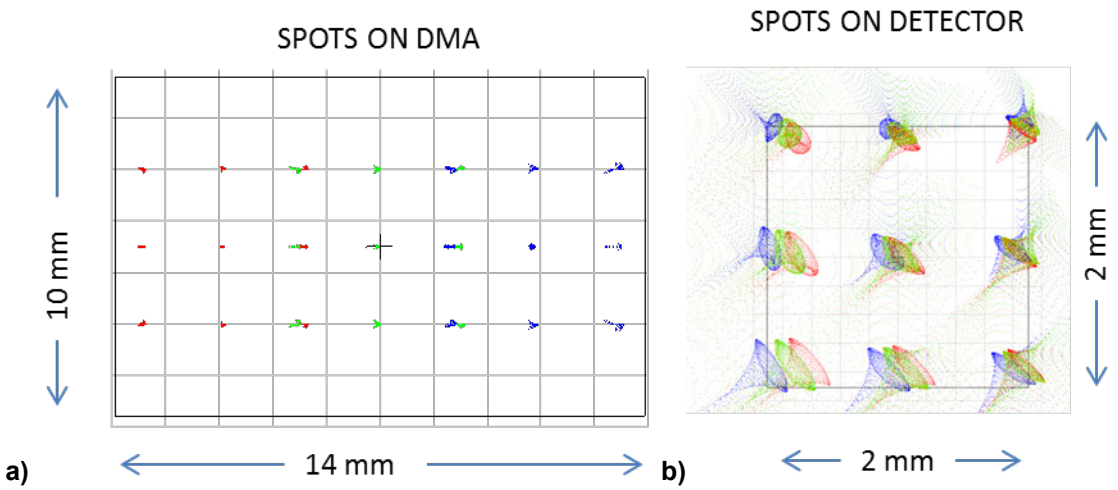

Figure 4. Spot diagram of the dispersed image with blue, 7.1 µm, green, 9.7 µm, red, 12.3 µm. left- on the DMA and right- on the detector

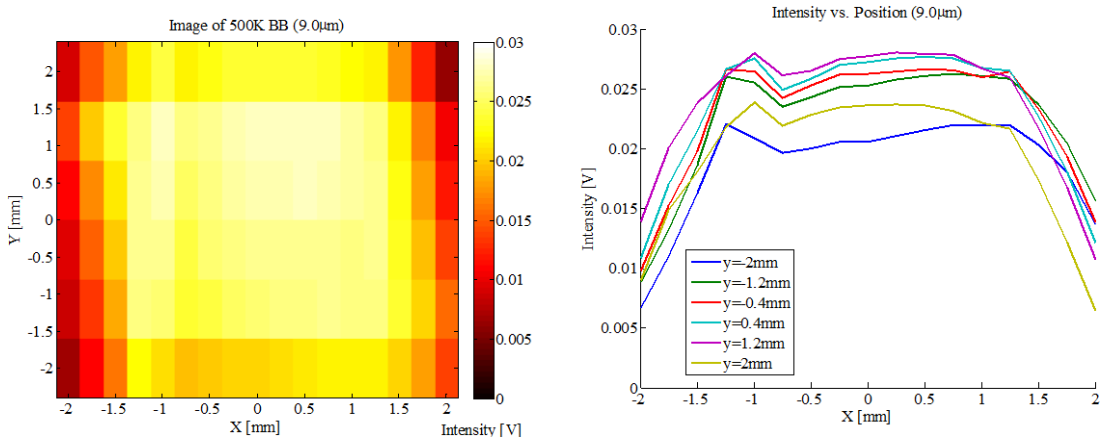

Figure 5. Observed intensity distribution across the input field of view in the 9 μm band.

4. IMAGE ENCODING

TRACER produces 2-dimensional imagery by combination of Hadamard multiplexing in the Y spatial dimension and slit scanning in the X direction. Figure 6 uses DMA spot diagrams to illustrate how spatial and spectral information is encoded using the slit and DMA. For any given slit position, the image spots along the slit dimension are dispersed across the DMA. The horizontal (X) direction is the spectral dimension, and the vertical (Y) dimension is the spatial dimension, along the slit. The slit is scanned horizontally to produce the second dimension of spatial imaging. This moves the dispersed image on the DMD in the X direction. For a single slit position, Hadamard multiplexing and spectral filters are used to encode the spatial/spectral image using the DMA. As the slit moves up and down, different parts of the image field are transmitted to the DMA, and the dispersed images shifts up and down on the DMA. Thus, different spectral encoding masks are needed for each slit position.

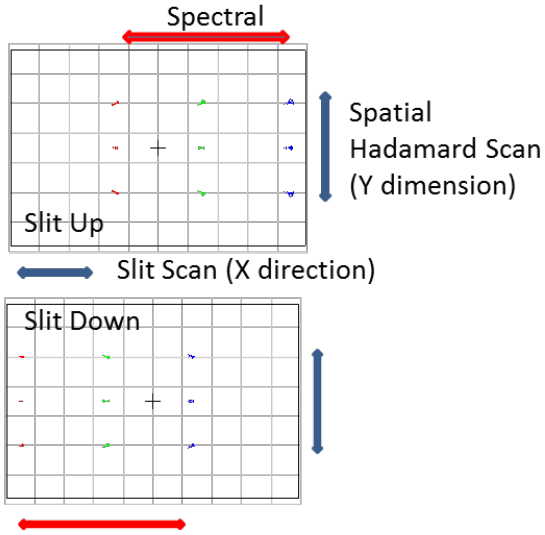

Figure 6. Spot diagram of the dispersed image on the DMA showing spatial and spectral scanning directions.

Spectral images are encoded as follows. For each slit position, M_i, the DMA is segmented into a two dimensional grid of superpixels, Sj, with each superpixel assigned to a predetermined wavelength. The minimum superpixel size is 8x16 DMA pixels, corresponding approximately to the resolution of the imaging optics. The superpixels are organized into N_k separately resolved regions which are scanned by Hadamard transform multiplexing. For each region, a set of F_l spectral filter masks are applied using grey scaling of the superpixels. The filter function can be as simple as an on and off filter for AC detection of the signal, or can be a complex spectral filter function generated with a linear combination of two or more analog spectral filter masks.

An example of contrast imaging with a spectral filter is illustrated in Figure 7. Hadamard transform spatial scanning is accomplished by organizing the N_k regions into H_k orthogonal Hadamard masks, with each mask containing a linear combination of spatial regions obtained by first ordering the regions into a vector and then applying the binary Hadamard cyclic simplex transform, [*H*].[6] The FPGA firmware then prepares a set of filter functions for each Hadamard mask and multiplies the Hadamard masks by the filter functions and applies them sequentially to the DMA. The resulting detector signals are then processed by first adding together the appropriately weighted signals corresponding to the filter masks and then reversing the Hadamard transform. The detector measures a signal equal to the product of the filter-function weighted incident intensity and the Hadamard mask transmission.

$$[D] = [H][FI], \tag{1}$$

where *[D]* is a column vector of *k* filter-weighted detector responses, *H,* is the encoding Hadamard

matrix, and, *[FI],* is the filter weighted column vector of intensities. The detector response, *[D],* is transformed into the intensity of the individual superpixels by applying the inverse Hadamard simplex matrix H^{-1}.

$$[FI] = [H\text{-}1\,][D] \tag{2}$$

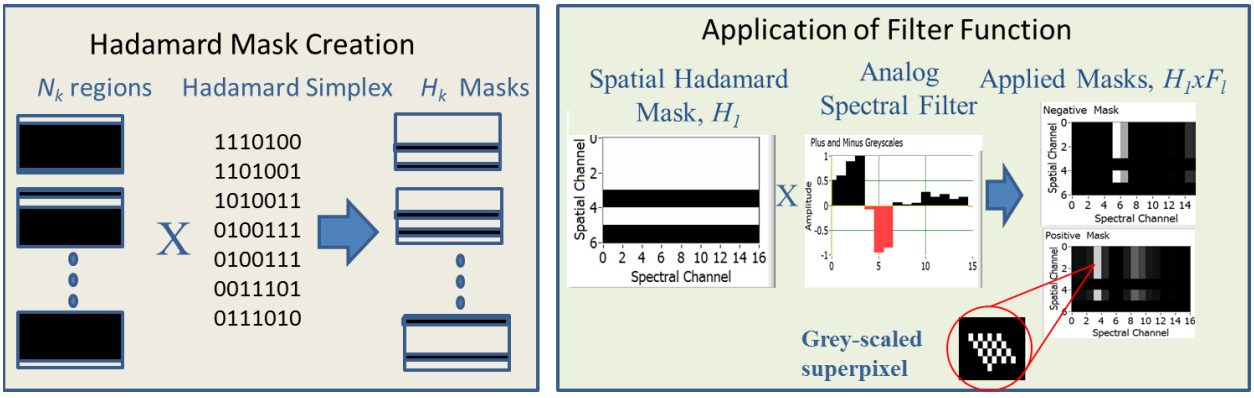

Figure 7. Production of filter-weighted Hadamard masks for chemical specific imaging.

The process is repeated for each of the slit positions, while scanning the slit and adjusting the position of the superpixels on the DMA to achieve the same spectral registration for every slit position as illustrated in Figure 6.

The time required to refresh an image is determined by the total number of masks used to generate the image. Table 1 shows typical operating parameters for the three modes of image formation, panchromatic imaging, Hadamard spectral imaging and chemical imaging. The image is refreshed at a rate of several Hz, and then averaged for a user selected integration period. The signal to noise of the resulting image is determined by the relative magnitude of the input image signal and the background-limited shot noise of the detector, which is typically 1.5×10^{-5} V/Hz$^{-1/2}$.

Table 1. Typical TRACER image formation parameters.

	Image Size Slit Dimension x Scan Dimension	**Spectral Dimension**	**# of Filters (F_i)**	**Image Refresh Rate @20kHz**
Panchromatic Thermal	36 x 28	1	2 (all-on, & all-off)	8 Hz
Chemical Imaging (Chemical-specific Contrast Imaging)	36 x 28	1	2 (all-on, & all-off)	8 Hz
Hadamard Spectral Imaging (Fast)	6 x 10	41	2 (Positive & Negative)	4 Hz
Hadamard Spectral Imaging (Hi Resolution)	12 x 28	41	2 (Positive & Negative)	0.7 Hz

Imaging Modes

The following section illustrates operation in the three imaging modes, Panchromatic Thermal, Chemical Imaging, and Hyperspectral imaging.

Figures 8 and 9 illustrate this process of image formation for the simplest case of a 2D panchromatic image. The figures illustrate the spatial resolution of the system. In these cases, the spatial regions are rows of superpixels, as in Figure 7, and the spatial filter encoding functions are 'all on' and 'all off', which leads to a chopped AC signal on the AC-coupled detector. The Y dimension contains N_k = 36 rows of superpixels which form the 4mm image area at the input image. The X dimension is scanned using M_i = 28, slit positions. In Figure 8, a hot wire point source is placed in the image field. In the X direction the resolution is limited by the size of the scanning slit, which is 300 microns wide. In the Y direction the FWHM is equal to the superpixel dimension, which is 8 pixels, or 106 microns. The halo observed around the hot wire is the reflection off the hot wire mount. Figure 9 shows a more complex panchromatic scene imaging result: a frozen bottle and a hot black body source partially obscured behind a metal panel 'test target' with holes. In this case we show the TRACER screen display, which includes a visible image of the scene on the left, along with the thermal IR image in false color. Images are shown with the zoom lens set for maximum field of view with focal length of 30 mm and zoomed in to the minimum field of view, with focal length of 100mm.

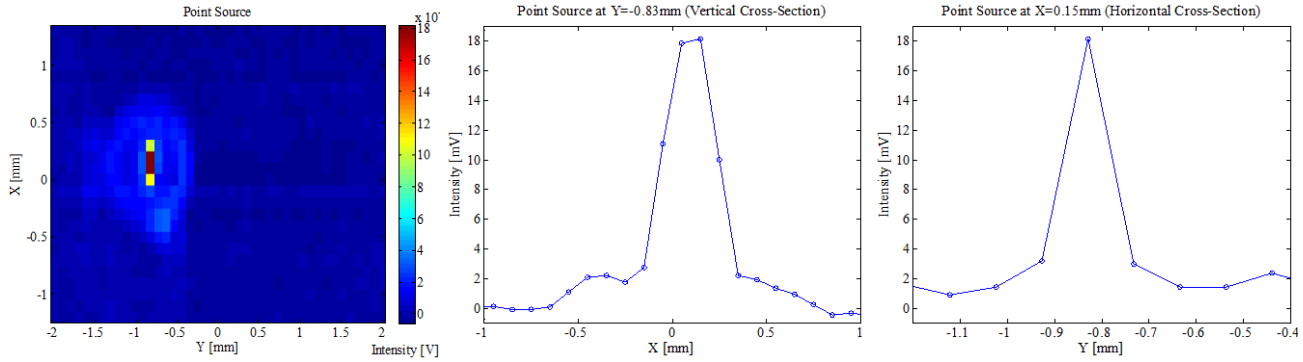

Figure 8. Image and intensity traces for a point object. Left-Image, Middle- X cross section, Right Y cross section.

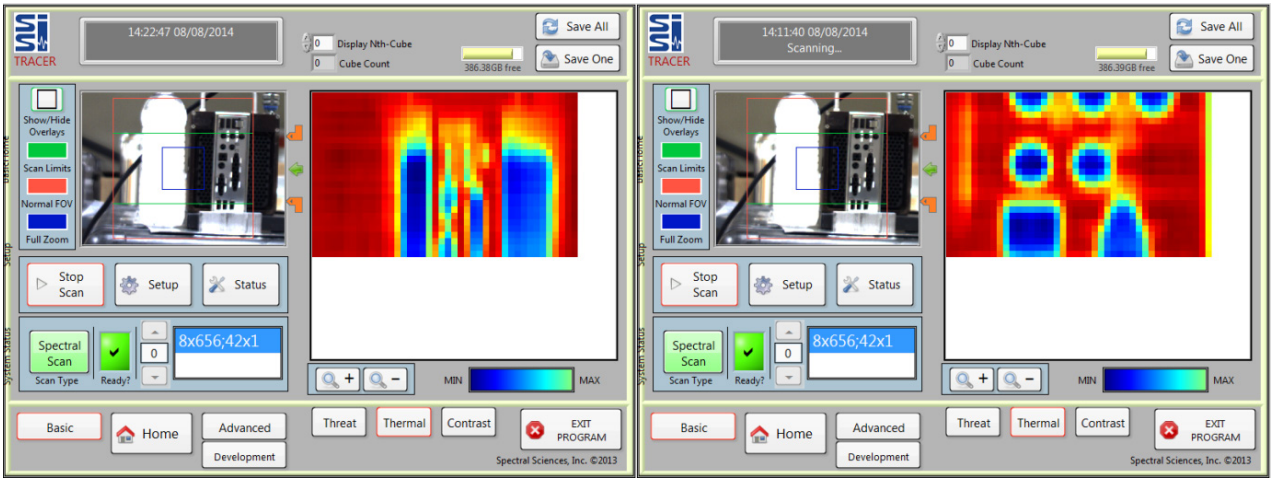

Figure 9. Screen shots of the TRACER display for thermal image tests. Left - wide angle including frozen bottle and test panel in front of blackbody, Right telephoto image of test target.

Figure 10 illustrates the results of 1D spectral/1D spatial Hadamard scans. Results are shown for a blackbody and the same blackbody viewed through a transmissive polystyrene standard. For spectral scans, the Hadamard transform scan is extended to both spectral and spatial dimensions by ordering the superpixels into a long vector containing, in this case, 6 spatial regions in the Y dimension of 8 superpixels each, and 41 spectral superpixels in the X direction. This vector is then subjected to the Hadamard transform and the all-on and all-off filter functions are applied. The detected signals are subtracted and the inverse transform is applied to obtain the absolute signal intensity in Volts for each spatial/spectral region. The process is then repeated for each row of the slit scan. Figure 10 shows the spectrum for each of the 6 Y regions observed with the slit at X = -1mm in the field of view. Scans are shown for a 500 degree blackbody target with, and without, a polystyrene film in front of it. The blackbody scans are used to calculate the absolute radiometric response function, by dividing the observed voltage by the known radiance of the blackbody target.

The measured polystyrene spectra of Figure 10 were used for wavelength calibration. The spectral dispersion was confirmed to be that calculated for the grating, which has a groove density of 14 grooves/mm. The spectral channels are separated by 129.7 nm/superpixel. The width of the polystyrene features confirm that the spectral resolution is determined primarily by the slit width of 300 microns, which is equivalent to 1.4 superpixels on the DMA. The spectral features of polystyrene are observed to have a FWHM of about 1.5 superpixels.

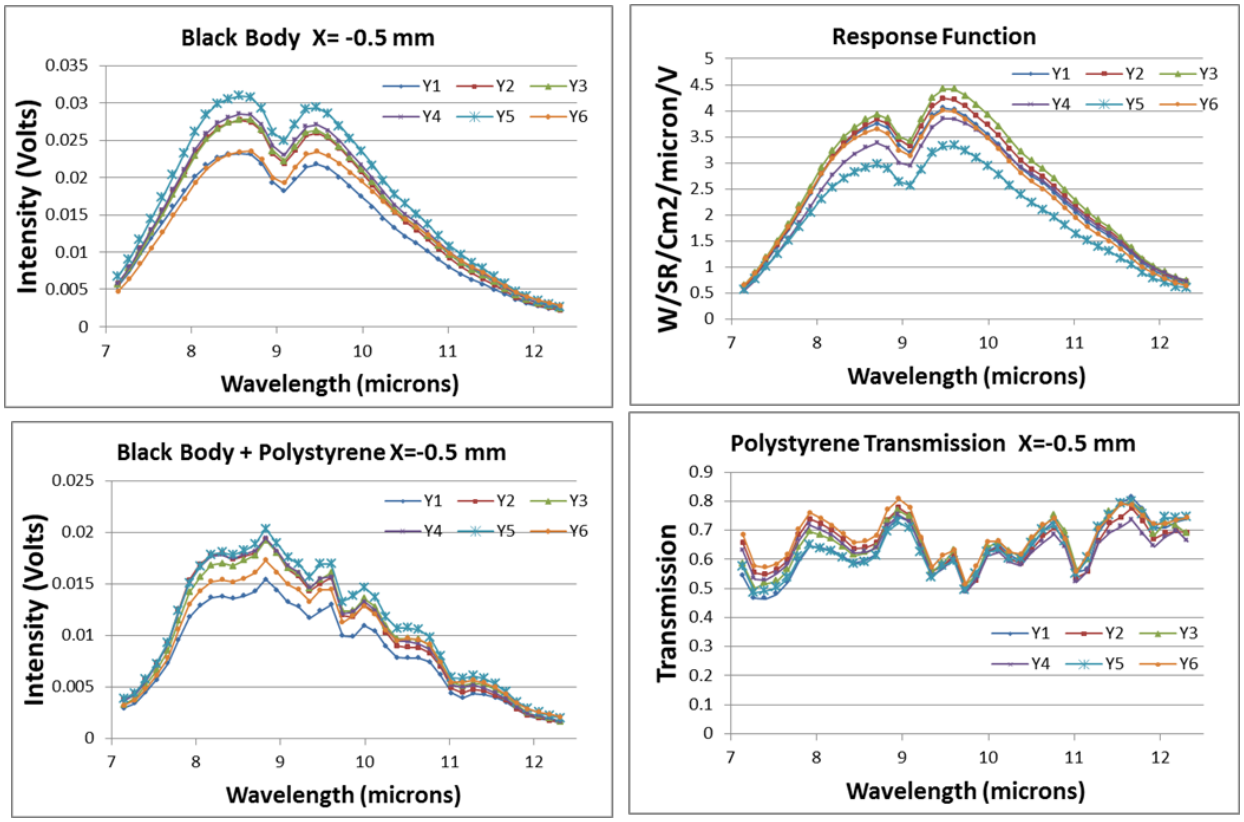

Figure 10. Spectral scans of blackbody target with and without polystyrene and resulting Response and transmission functions.

Figure 11 illustrates the production of a chemical image using an analog contrast filter. A contrast filter scan is similar to a 2D panchromatic image scan, in that the rows of the DMA are organized as Hadamard masks, as shown in Figure 7. In this case however, the filter function applied along the spectral dimension is a matched filter for polystyrene in the presence of blackbodies. The polystyrene and blackbody spectra of Figure 10 are used to generate a generalized matched filter according to the methodology outlined in previous work.[5] The positive and negative filter masks are applied in succession using superpixel greyscales, and the detector signal is subtracted and Hadamard transformed to form the rows of the image shown in Figure 11. The slit is scanned to produce the columns of the image.

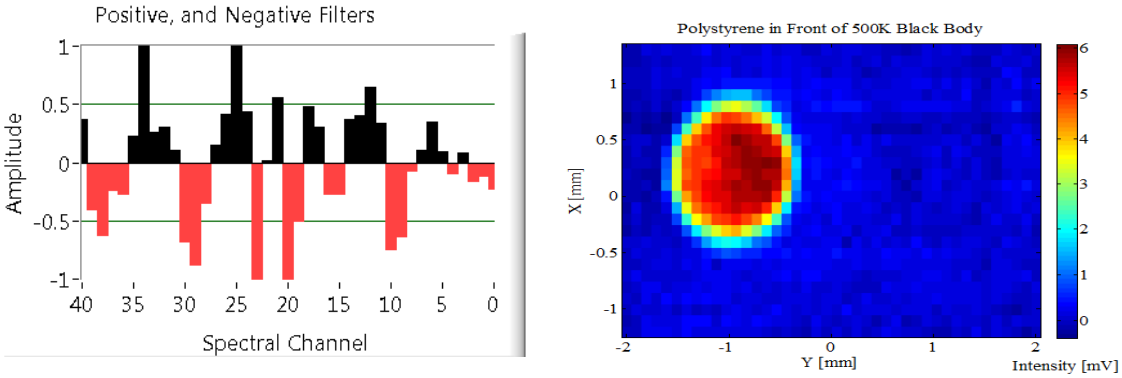

Figure 11. Contrast image of polystyrene in front of a Blackbody. Left Contrast filter function. Right – observed contrast image.

5. APPLICATION TO FLAME MONITORING

TRACER has general utility in monitoring gases, liquids and solids through detection and analysis of spectral signatures. We report here as an example of spectral characterization and contrast imaging of the exhaust from a laboratory burner. Figure 12 shows a picture of the set-up. The TRACER system is mounted on a tripod and pointed at the exhaust of a four-burner premixed combustor. The combustor has a quartz exhaust duct, designed for visual characterization of the flame. Since quartz is opaque in the long-wave infrared, TRACER is set up to monitor the exhaust at the exit of the quartz duct. Figure 13 shows some examples of the observed spectra of the flame and of the quartz exhaust duct. These spectra are shown as raw voltages and have not been scaled by the response function of Figure 10. Such raw spectra are used to make the chemical detection filters, as the application of the filter takes place in hardware, and detector response is in measured voltage, not the radiant intensity of the source. The left hand side shows the spectra observed at the exit of the combustor. The flame spectra show the characteristic emission of H_2O and water. The quartz spectrum, which is almost two-orders of magnitude brighter, is similar in shape to the blackbody of Figure 9, but with a large bite-out at 9 microns, where quartz has a strong reflectance feature. The spectra of Figure 13 were used to construct a generalized matched-filter for detection of the flame and rejection of the quartz. Figure 14 shows the resulting filter masks used for flame imaging.

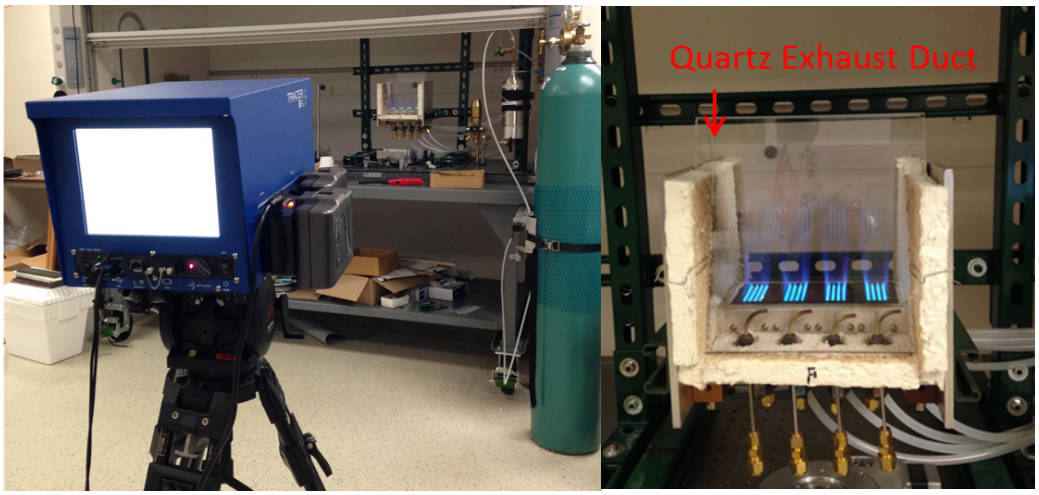

Figure 12. Setup for flame measurements. Left – TRACER position. Right – Premixed burner with quartz exhaust duct.

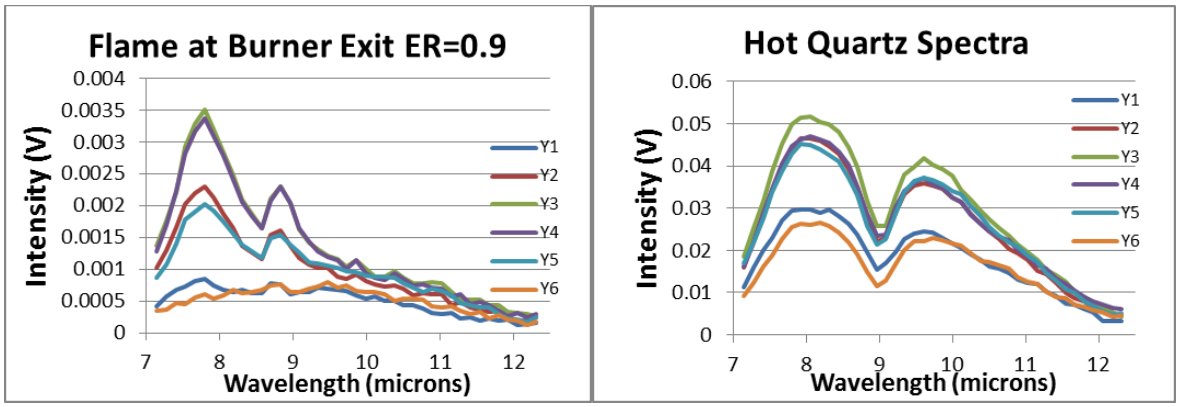

Figure 13. Flame and quartz spectra. Left – flame at six spatial positions just above the exhaust duct.. Right – quartz exhaust duct.

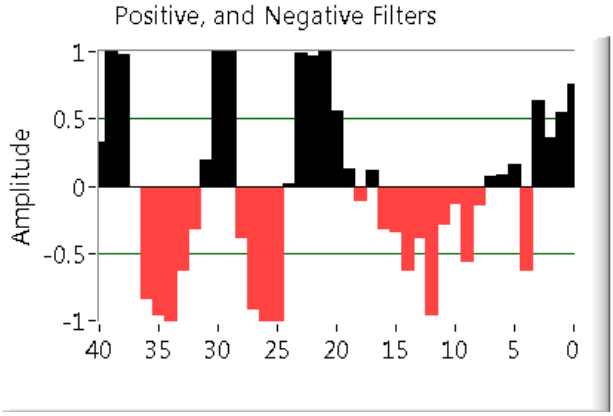

Figure 14. Spectra of hot quartz chimney and matched filter.

The spectra of Figures 12 and 13 were recorded by dividing the horizontal field (Y direction) into 6 spatial regions with different amounts of hot exhaust. The central two regions see the brightest flame with the hottest water, while the outermost regions see little flame and colder water emission. Figure 15 shows spectra observed in central, Y3, region as a function of flame equivalence ratio. (Equivalence ratio is a scaled fuel/air ratio where ER=1 means stoichiometric combustion. ER>1 is a rich flame and ER<1 is a lean flame.) The exhaust spectra are seen to be similar in shape, but the overall intensity increases with equivalence ratio.

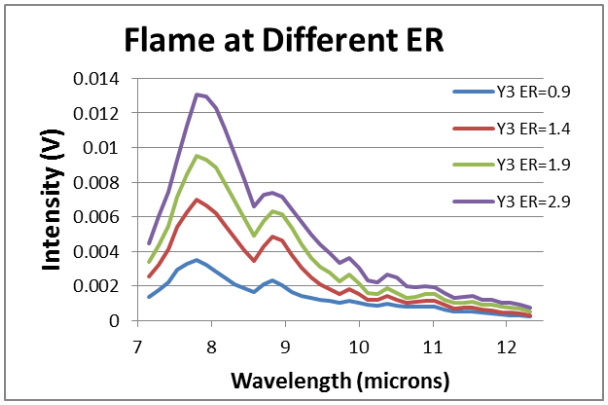

Figure 15. Flame spectra as a function of Equivalence Ratio (ER).

Figure 16 shows a comparison of the observed spectrum to that predicted for CO_2 and water, based on a simplified model. The calculated spectra are scaled by the response function to compare them to the observed spectra. The water spectrum is observed in the grating's first order and is due primarily to the water band centered at 6.3 microns. The CO_2 spectrum arises from the 4.2 micron CO2 band and is centered at 4.5 microns. It and is observed in the grating's second order. Because the grating is blazed for 9 microns, the second order diffraction is the most intense order for this band. The spectrum of hot CO_2 and H2O is well known, but the details of the observed spectrum depend on the temperature distribution of the boundary region of the flame since centers of the water and CO_2 line can be optically thick. The basic features of the spectrum can be reproduced with a simplified model, in which we assumed three layers of constant temperature, a central hot layer (1200K) 3 cm in length, a 1 cm long layer at intermediate temperature (500 K), and 2.7 m of room temperature air between the flame and the sensor. This model is sufficient to capture most of the features observed in the flame. The intensity of the observed radiation and the location of the water band edge between 7 and 8 microns suggest a core temperature of about 1200K.

The overlap of the first and second order spectra can be useful in cases such as these, where we are interested in detecting both wavelength regions. In other cases, they might be a cause of confusion. In such cases, a band-pass filter is added to the optical path.

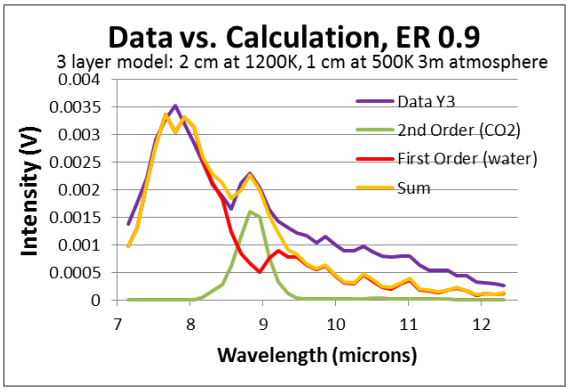

Figure 16. comparison of observed and calculated flame spectra.

Flame Contrast Imagery

Figures 17 and 18 show panchromatic thermal images, and flame matched-filter contrast images obtained in contrast imaging mode. In each case we collect a 28x36 image by scanning the slit through 28 positions and using Hadamard multiplexing over 36 rows of superpixels. For the panchromatic image, a set of all-on and all-off masks are applied. For the flame contrast image, the filter masks of Figure 14 are applied. Figure 16 shows screen shots of the TRACER user interface for each of these cases. The interface shows a visual image of the flame alongside a false color infrared contrast image. The left hand side shows the display for the panchromatic image, the right-hand side shows the display for the flame matched-filter contrast image.

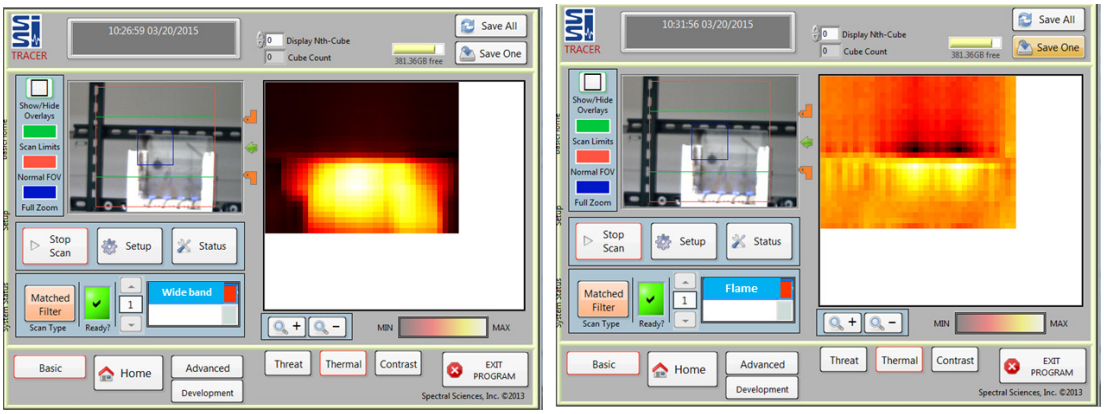

Figure 17. TRACER display of panchromatic thermal image and flame matched-filter contrast image.

Figure 18 shows the same data plotted as contour plots for ease of viewing. The outline of the quartz exhaust duct is clearly visible in the panchromatic thermal image, while the flame is clearly visible in the flame matched-filter contrast image and the quartz is rejected. Note that the total emission signal from the quartz is nearly two orders of magnitude larger than that of the flame emission. The spectral matched filter is able to suppress the quartz background signal while recognizing the spectral signature of the flame.

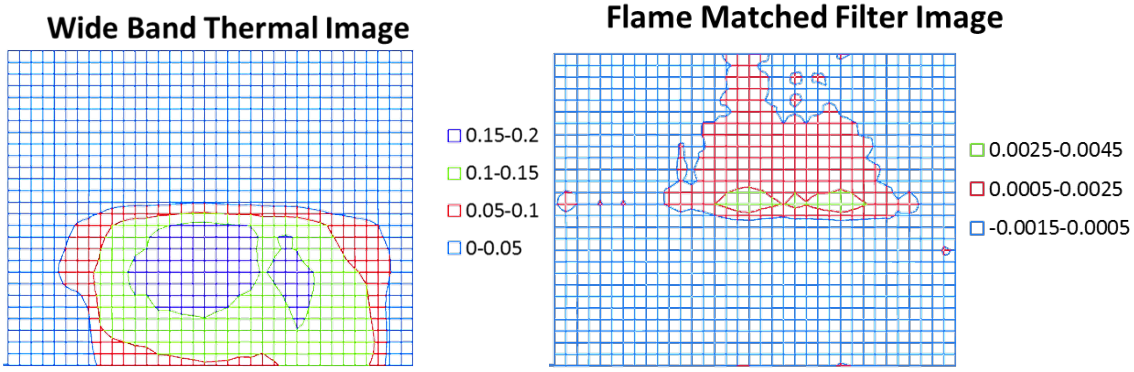

Figure 18. Contour plots of wide-band thermal image intensity and flame matched-filter contrast image response.

6. SUMMARY AND CONCLUSIONS

We have built and demonstrated a tripod mounted spectral imager for detection of effluents and surface residues. Operation in a variety of modes, including panchromatic thermal imaging, Hadamard-multiplexed hyperspectral imaging and chemical-specific contrast imaging has been demonstrated. All three modes would be useful in a measurement campaign. Panchromatic thermal imagery rapidly provides gross context of the scene, hyperspectral imagery measures complex spectral features of materials in the scene, and contrast imagery rapidly detects trace species of effluent. The ability to switch between modes rapidly allows the user to respond to changing measurement needs. The value of the sensor for rapidly detecting trace species for process monitoring applications, such as the flame exhaust above the quartz duct, was shown.

ACKNOWLEDGEMENT

The authors gratefully acknowledge the Defense Threat Reduction Agency for funding the development of the the TRACER sensor under contract HDTRA1-12-C-0095 and Spectral Science Inc. for Internal IR&D funding of the effluent measurements reported herein.

REFERENCES

[1] Fox, M.J., Goldstein, N., Vujkovic-Cvijin, P., Gregor, B., Adler-Golden, S., Cline, J., St. Peter, B., Lowell, A. and Wilder, M., "A compact, thermal-infrared spectral imager for chemical-specific detection," Proc. SPIE 8870, Imaging Spectrometry XVIII, 887004 (2013).

[2] Goldstein, N., St. Peter, B., Fox, M.J., Grot, J., Kogan, M. and Brancazio, D., Thermal infrared Reconfigurable Analysis Camera for Effluents and Residues (TRACER) Final Technical Report, (2014).

[3] Goldstein, N., Vujkovic-Cvijin, P., Fox, M. J., Adler-Golden, S., Lee, J., Cline, J.A., Gregor, B., "Spectral Encoder," US Patent 7,324,196 (2008).

[4] Goldstein, N., Vujkovic-Cvijin, P., Fox, M.J., Gregor, B., Lee, J., Cline, J., and Adler-Golden, S., "DMA-based adaptive spectral imagers for hyperspectral imagery and direct detection of spectral signatures," SPIE Vol. 7210, paper 721008-8 (2009).

[5] Goldstein, N., Fox, M.J., Adler-Golden, S. and Gregor, B., " Infrared adaptive spectral imagers for direct detection of spectral signatures and hyperspectral imagery ," Proc. SPIE 8618, Emerging Digital Micromirror Device Based Systems and Applications V, 8618-12 (2013).

[6] Harwit, M. and Sloane, N.J.A., Hadamard Transform Optics, Academic Press, NY, (1979).